Effects of nonlocalized target shape in the random walk description of transillumination experiments for optical imaging

George H. Weiss[1] and Amir H. Gandjbakhche[2]
[1]*Physical Sciences Laboratory, Division of Computer Research and Technology, National Institutes of Health, Bethesda, Maryland 20892*
[2]*Office of the Director, National Institute of Child Health and Human Development, National Institutes of Health, Bethesda, Maryland 20892*
(Received 28 March 1997)

A lattice random walk theory has been successfully used to interpret and analyze a variety of experimental data related to applications in optical imaging. A major advantage of the lattice theory is that it replaces cumbersome eigenfunction expansions resulting from diffusion theory by simpler relations expressed in terms of generating functions. The transillumination experiment has previously been analyzed by representing a region of increased absorptive properties in tissue by a single anomalous point. Here we extend the analysis to allow for k anomalous sites, thus providing a tool for studying the effects of nonlocality of the anomalous region. We show that if the absorption coefficient in the anomalous region is sufficiently small, the simple approximation based on the use of a single point with an anomalous absorption coefficient yields quite good results as compared to data obtained from phantoms. It is shown that the neglect of correlation effects leads to an underestimate of the absorption coefficient in an anomalous region. [S1063-651X(97)12109-2]

PACS number(s): 87.10.+e, 05.40.+j

I. INTRODUCTION

Many research groups are presently exploring the possible use of optical methods as a tool for clinical imaging, and a vast literature on this subject has been produced, cf., for example [1,2]. Optical techniques are attractive as a biomedical tool because they do not involve the use of ionizing radiation. Optical imaging techniques depend on there being a difference between optical properties of an embedded abnormal body and those of the tissue surrounding it. These differences may be in the absorption or scattering coefficients, or both. At the same time a major drawback to successfully implementing optical methods is the lesser degree of resolution obtainable as compared to that associated with x-ray imaging techniques. This is attributable to multiple scattering of the photons by tissue inhomogeneities, which produces image blurring. This negative effect can be partially overcome in transmission imaging by using time-gated transillumination experiments, (cf. Fig. 1). In the implementation of transillumination measurements the role of time gating is to select photons that arrive at the detector at the earliest possible times. This selection is equivalent to utilizing those photons whose paths are most localized spatially in traversing the tissue, and which not have had time to diffuse by an appreciable amount.

The design of imaging instrumentation based on time gating requires choosing the time-gating period. Too short a period results in the image being dominated by noise. In addition, the fact that the photon intensity is necessarily quite low at very short times is a negative factor to be considered in clinical applications of such technology. On the other hand, too long a gating time, although providing an adequately detectable number of photons, degrades both contrast and resolution due to wandering due to diffusion. In order to examine questions related to the tradeoffs involved in choosing the time-gating period it is necessary to model the kinetics of photon migration in a turbid medium. Many analytical and numerical approaches have been used in an attempt to solve this problem to balance the accuracy of a rigorous physical model with the convenience of a more approximate one requiring a simpler mathematical formalism for its exploitation. From the physical viewpoint the most accurate class of models for this purpose are those based on the solution of a full transport equation, but such equations are only solvable numerically for realistic problems. Also, neither the form nor the parameters that define the scattering

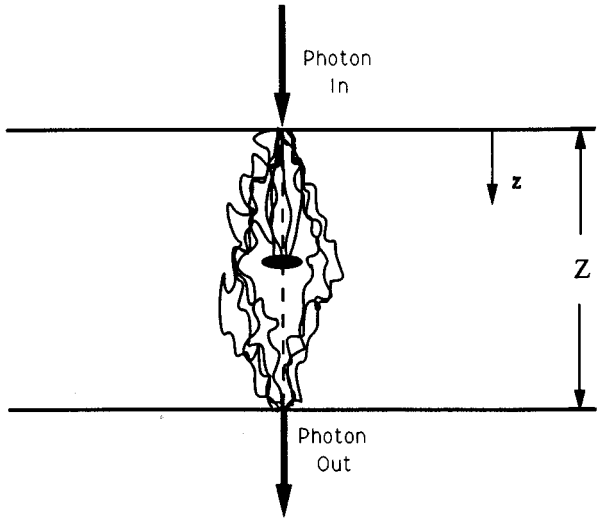

FIG. 1. Schematic diagram of the transillumination experiment. In our analysis of the coaxial experiment the source and detector are taken to be collinear with the center of the anomalous region. If the detector is moved relative to the source the numerical results would be qualitatively similar.

kernel are known to any degree of precision. Because of these difficulties the analysis of photon migration in a turbid medium is often based on the use of considerably simplified phenomenological models whose utility is measured by how well they produce results in accord with experiments.

An obvious candidate for a simplified model of photon motion is the standard diffusion process, which has indeed been used successfully by many investigators, [3–5]. Diffusion models, however, have the negative feature that solving a problem with an inclusion and with boundaries requires the solution of a generally quite complicated boundary-value problem, as exemplified by analysis in the paper by den Outer, Niewenhuizen, and Lagendijk [6]. An alternative to a diffusion-theory-based model is one based on the discrete-time lattice random walk [7,8]. Random walk models have successfully been used to reconstruct images from experimental data obtained from measurements using phantoms [9]. Further, the central-limit theorem guarantees that many results derived from the theory of random walks will agree, after proper scaling, with those derived from diffusion theory [10].

Relevant to the present discussion is that a formalism based on the lattice random walk model can simplify problems that involve inclusions because the boundary value problems for the diffusion equation are replaced by problems that require dealing only with discrete quantities. A further advantage of this formulation accrues from the fact that many random walk problems are solvable in terms of generating functions. Such solutions are applicable, without further approximation, to interpret results obtained using frequency-domain spectroscopy.

An example in which the random walk formalism has been used appeared recently in a study of absorptivity contrast in transillumination imaging of tissue inclusions [11]. This investigation, as well as more recent ones on reflection experiments as used in fluorescence spectroscopy [12,13], approximated the anomalous region by a single lattice point. In an earlier application based on random walk methodology we used an ad hoc approximation that omitted all correlations, by which we mean the possibility of photons hopping between different anomalous sites. This artifice allowed us to take into account differently shaped sets of anomalous points without unduly complicating the necessary numerical computations [9]. The analysis to follow is aimed at an approximate assessment of the penalty incurred by neglecting these correlations.

In this paper we deal with a case in which the anomalous points have absorption coefficients that differ from those of the master lattice whose properties model the normal tissue. When NIR radiation is used for imaging purposes experimental values of the absorption coefficient with an anomalous site tends to be very small when expressed in dimensionless units. This circumstance allows us to exploit a perturbation expansion of the exact generating function that facilitates examining the difference between the propagator in the presence and absence of the set of anomalous sites. In particular, this study is aimed at assessing correlation effects and at incorporating these effects, at least approximately, into the analysis. We will assume that the absorptivity of points outside of the anomalous set is negligible, and will accordingly be set equal to zero. The theory is easily generalized to allow for absorption on nonanomalous sites.

II. ANALYSIS

A. General formalism

The slab of tissue shown in Fig. 1 is modeled as a simple cubic lattice bounded by two parallel planes. The coordinates of an arbitrary point on the lattice will be denoted by $\mathbf{r}=(x,y,z)$, the components of which are integers that satisfy $-\infty\leqslant x,y\leqslant\infty$ and $0\leqslant z\leqslant Z$. Our use of integer units is convenient for the following analysis; later we indicate how to convert the results to physical units. The set of anomalous points will be denoted by $S=(\mathbf{s}_1,\mathbf{s}_2,\ldots,\mathbf{s}_k)$. The two parallel interfaces that define the slab, $z=0$ and $z=Z$, will be assumed to consist only of absorbing points so that a photon that reaches one or the other of the two faces is instantly absorbed there. The initial position of an injected photon will be denoted by $\mathbf{r}_0=(0,0,1)$ so that the lattice spacing is of the order of a scattering length. Photon motion will be modeled in terms of an isotropic random walk on a simple cubic lattice. The random walk will be allowed to take steps to nearest neighboring sites only, so that the probability that a photon moves to a particular neighboring site in a single step is equal to $\frac{1}{6}$. We seek to determine the number and distribution of photons that reach $z=Z$ at step n in the presence of the set S.

The probability that a photon, on hitting a site belonging to S, is absorbed at that site will be denoted by η so that $\eta=1$ corresponds to a completely absorbing site. To simplify our analysis we will assume that the absorption probability of any site not in S is equal to zero. This is realistic since when NIR radiation is used the values of η tend to be rather small (typical values are between 0.01 and 0.05 [14]). This feature will be exploited to develop a perturbation expansion of the exact solution. Other alternatives require rather cumbersome calculations.

A complete description of photon motion is contained in two sets of probabilities: $\{p_n(\mathbf{r}|\mathbf{r}_0)\}$ and $\{q_n(\mathbf{r}|\mathbf{r}_0)\}$. The function $p_n(\mathbf{r}|\mathbf{r}_0)$ is the probability that a photon on a lattice slab with absorbing boundaries moves from the site $\mathbf{r}_0$ to $\mathbf{r}$ in n steps when there are no anomalous sites. The function $q_n(\mathbf{r}|\mathbf{r}_0)$ is the probability that the photon moves from $\mathbf{r}_0$ to $\mathbf{r}$ in n steps, taking both the absorbing interfaces and the anomalous sites into account. This latter set of probabilities is the one required to describe the physics inherent in our particular problem, but the $q_n(\mathbf{r}|\mathbf{r}_0)$ can be expressed in terms of the $p_n(\mathbf{r}|\mathbf{r}_0)$, for which exact expressions are available [10].

In the lattice random walk model the flux of photons into a site $\mathbf{r}=(x,y,Z)$ at the nth step of the random walk is

$$\mathbf{J}_n(\mathbf{r})=q_{n-1}(x,y,Z-1|0,0,1)/6 \tag{2.1}$$

since, in order to reach $\mathbf{r}$ at step n the photon must reach $(x,y,Z-1)$ at step $n-1$, the nth step taking it from $Z-1$ to Z with probability 1/6. Hence we see that the flux is directly related to the state probability $q_n(\mathbf{r}|\mathbf{r}_0)$. The two sets of probabilities are not easily related to one another, but their generating functions are.

The generating function of an arbitrary sequence $\{g_n\}$ will be denoted by $\hat{g}_\xi$, which is

$$\hat{g}_\xi = \sum_{n=0}^{\infty} g_n e^{-n\xi}. \tag{2.2}$$

A relation between $\hat{q}_\xi(\mathbf{r}|\mathbf{r}_0)$ and $\hat{p}_\xi(\mathbf{r}|\mathbf{r}_0)$ can be established following the analysis in [16]. That paper contains a calculation of the n-step propagator for a random walk conditional on the number of visits to sites in a set S, a function that will be denoted by $p_n(\mathbf{r}|\mathbf{r}_0;\mathbf{l})$. More precisely, these are the n-step propagators conditional on making l_1 visits to $\mathbf{s}_1$, l_2 visits to $\mathbf{s}_2$, and so forth. These probabilities cannot be found directly. However, it is possible to find an explicit expression for the related generating function

$$\Gamma(\mathbf{r}|\mathbf{r}_0;\boldsymbol{\alpha},\beta) = \sum_{n=0}^{\infty} \beta^n \sum_{l_1=0}^{\infty} \cdots \sum_{l_k=0}^{\infty} p_n(\mathbf{r}|\mathbf{r}_0;\mathbf{l}) \alpha_1^{l_1} \alpha_2^{l_2} \cdots \alpha_k^{l_k}, \tag{2.3}$$

where the α_i and β are variables that define the generating function. To translate this form of the generating function into the form required in the present paper one notes that in order for the photon to reach $\mathbf{r}$ at step n it is necessary that no visit to S should have resulted in the photon being absorbed there. This requirement is expressible in terms of $\Gamma(\mathbf{r}|\mathbf{r}_0;\boldsymbol{\alpha},\beta)$ as defined in Eq. (2.3) by setting $\alpha_i = 1-\eta$, $i(\neq j) = 1,2,\ldots,k$. To complete the transition from the generating function in Eq. (2.3) to an equivalent one for the $q_n(\mathbf{r}|\mathbf{r}_0)$ one sets $\beta = \exp(-\xi)$.

To simplify notation we abbreviate the generating functions for transitions between sites in S with no anomalous sites as

$$\hat{p}_{\xi,ij} \equiv \hat{p}_\xi(\mathbf{s}_i|\mathbf{s}_j). \tag{2.4}$$

The desired relation has been shown to be expressible as

$$\hat{q}_\xi(\mathbf{r}|\mathbf{r}_0) = \begin{cases} \hat{p}_\xi(\mathbf{r}|\mathbf{r}_0) - \eta \displaystyle\sum_{j=1}^{k} \frac{D_j(\xi,\eta)}{D(\xi,\eta)} \hat{p}_\xi(\mathbf{r}|\mathbf{s}_j), & \mathbf{r} \notin S \\ (1-\eta)\, \dfrac{D_j(\xi,\eta)}{D(\xi,\eta)}, & \mathbf{r} \in S \end{cases} \tag{2.5}$$

in [15]. In this equation $D(\xi,\eta)$ is the $k \times k$ determinant

$$D(\xi,\eta) = \begin{vmatrix} 1+\eta(\hat{p}_{\xi,11}-1) & \eta\hat{p}_{\xi,12} & \cdots & \eta\hat{p}_{\xi,1k} \\ \xi\hat{p}_{\xi,21} & 1+\eta(\hat{p}_{\xi,22}-1) & \cdots & \eta\hat{p}_{\xi,2k} \\ \vdots & \vdots & \ddots & \vdots \\ \eta\hat{p}_{\xi,k1} & \eta\hat{p}_{\xi,k2} & \cdots & 1+\eta(\hat{p}_{\xi,kk}-1) \end{vmatrix} \tag{2.6}$$

and $D_j(\xi,\eta)$ is found from $D(\xi,\eta)$ by replacing column j by a vector whose lth component is $\hat{p}_\xi(\mathbf{s}_l|\mathbf{r}_0)$. In the case of a single anomalous site at $\mathbf{s}$, Eq. (2.5) reduces to

$$\hat{q}_\xi(\mathbf{r}|\mathbf{r}_0) = \hat{p}_\xi(\mathbf{r}|\mathbf{r}_0) - \eta \frac{\hat{p}_\xi(\mathbf{r}|\mathbf{s})\hat{p}_\xi(\mathbf{s}|\mathbf{r}_0)}{1+\eta[\hat{p}_\xi(\mathbf{s}|\mathbf{s})-1]}, \tag{2.7}$$

which is the result used in [11] and which can be derived without resorting to the more general analysis in [15].

The contrast function at step n measured at a point on the boundary $\mathbf{r} = (x,y,Z)$ will be denoted by $C_n(\boldsymbol{\rho}|\mathbf{r}_0)$, where $\boldsymbol{\rho}$ is the two-dimensional vector (x,y). It is defined as

$$C_n(\boldsymbol{\rho}|\mathbf{r}_0) = 1 - \frac{q_n(\boldsymbol{\rho}|\mathbf{r}_0)}{p_n(\boldsymbol{\rho}|\mathbf{r}_0)} \tag{2.8}$$

and is a measure of the change in the flux induced by the presence of a set of absorbing sites. On returning to Eq. (2.5) we see that the contrast function can be expressed in the general form

$$C_n(\boldsymbol{\rho}|\mathbf{r}_0) = \eta \frac{\sum_{j=1}^{k}\sum_{l=0}^{n} A_l^{(j)}(\boldsymbol{\rho},\mathbf{s}_j) p_{n-l}(\mathbf{r}|\mathbf{s}_j)}{p_n(\boldsymbol{\rho}|\mathbf{r}_0)}, \tag{2.9}$$

in which the functions $A_m^{(j)}(\boldsymbol{\rho},\mathbf{s}_j)$ are found as the inverse of the generating functions $D_j(\xi,\eta)/D(\xi,\eta)$ regarded as a function of ξ. It is not generally possible to calculate these inverses in closed form. However, taking advantage of the fact that η is small for applications involving NIR radiation, we can expand both $D_j(\xi,\eta)$ and $D(\xi,\eta)$ in a perturbation series, from which one can obtain approximations to the $A_m^{(j)}$ that appear in Eq. (2.9).

Before discussing some of the implications of the perturbation expansion we introduce what will be referred to as the additive-sites model, which neglects all correlation effects, and uses the further approximation that all of the diagonal terms in $D(\xi,\eta)$ are equal. This last assumption is quite accurate provided that the anomalous sites are not located within one or two lattice spacings from either of the boundaries. Accordingly we set $\hat{p}_{\xi,11} = \hat{p}_{\xi,22} = \cdots = \hat{p}_{\xi,kk} = \hat{p}_{\xi,d}$. Both $D(\xi,\eta)$ and $D_j(\xi,\eta)$ can be found in closed form for the additive-sites model:

$$D(\xi,\eta) = [1+\eta(\hat{p}_{\xi,d}-1)]^k,$$
$$D_j(\xi,\eta = \hat{p}_\xi(\mathbf{s}_l|\mathbf{r}_0)[1+\eta(\hat{p}_{\xi,d}-1)]^{k-1}. \tag{2.10}$$

But this means that

$$\frac{D_j(\xi,\eta)}{D(\xi,\eta)} = \frac{\hat{p}_\xi(s_l|r_0)}{1+\eta(\hat{p}_{\xi,d}-1)}. \tag{2.11}$$

In the additive-sites model the relation between the generating function for the propagator allowing for anomalous sites and the propagator for the homogeneous lattice is

$$\hat{q}_\xi(\mathbf{r}|\mathbf{r}_0)\approx\hat{p}_\xi(\mathbf{r}|\mathbf{r}_0)-\eta\,\frac{\hat{W}_\xi(\mathbf{r}|\mathbf{r}_0;S)}{1+\eta(\hat{p}_{\xi,d}-1)}. \tag{2.12}$$

Here we have written

$$\hat{W}_\xi(\mathbf{r}|\mathbf{r}_0;S)=\sum_{j=1}^{k}\hat{p}_\xi(\mathbf{r}|\mathbf{s}_j)\hat{p}_\xi(\mathbf{s}_j|\mathbf{r}_0), \tag{2.13}$$

the time-domain equivalent of this relation being

$$W_n(\mathbf{r}|\mathbf{r}_0;S)=\sum_{j=1}^{k}\sum_{l=0}^{n}p_l(\mathbf{r}|\mathbf{s}_j)p_{n-l}(\mathbf{s}_j|\mathbf{r}_0). \tag{2.14}$$

Thus, the approximation in Eq. (2.12) neglects events in which a photon hops from one of the anomalous sites to another. In the remainder of the paper we use a perturbation expansion of the result in Eq. (2.5) to explore some consequences of including such events.

B. The perturbation expansion

Here we consider the detailed form of the expansions of $D(\xi,\eta)$ and $D_j(\xi,\eta)$ around $\eta=0$. The first two terms in the expansion of $D(\xi,\eta)$ are

$$\begin{aligned}D(\xi,\eta)\approx 1+\eta\sum_{j=1}^{k}[(\hat{p}_{\xi,jj}-1)]\\ +\frac{\eta^2}{2}\sum_{i(\neq j)=1}^{k}\sum_{j=1}^{k}\{(\hat{p}_{\xi,ii}-1)(\hat{p}_{\xi,jj}-1)\\ -\hat{p}_{\xi,ij}\hat{p}_{\xi,ji}\}+\cdots .\end{aligned} \tag{2.15}$$

Since properties of the random walk are assumed to be isotropic the correlation terms are symmetric in the sense that $\hat{p}_{\xi,ij}=\hat{p}_{\xi,ji}$. Similarly, the lowest order terms in the expansion of $D_j(\xi,\eta)$ are

$$\begin{aligned}D_j(\xi,\eta)\approx\hat{p}_\xi(\mathbf{s}_j|\mathbf{r}_0)+\eta\Bigg\{\hat{p}_\xi(\mathbf{s}_j|\mathbf{r}_0)\sum_{i(\neq j)=1}^{k}[\hat{p}_{\xi,ii}-1]\\ -\sum_{i(\neq j)=1}^{k}\hat{p}_\xi(\mathbf{s}_i|\mathbf{r}_0)\hat{p}_{\xi,ij}\Bigg\}.\end{aligned} \tag{2.16}$$

Two observations should be made at this point. First, we observe that if the expansion of $D(\xi,\eta)$ is truncated at the first order in η and only the leading term in $D_j(\xi,\eta)$ is retained, the approximation to Eq. (2.5) for $\mathbf{r}\notin S$ will have the same functional form as Eq. (2.7) except that the term $[\hat{p}_\xi(\mathbf{s}|\mathbf{s})-1]$ in that equation is replaced here by the sum $\Sigma_{j=1}^{k}(\hat{p}_{\xi,jj}-1)$. As mentioned earlier, we can set $\hat{p}_{\xi,jj}\approx\hat{p}_{\xi,d}$ so that the sum reduces to

$$\sum_{j=1}^{k}(\hat{p}_{\xi,jj}-1)\approx k(\hat{p}_{\xi,d}-1). \tag{2.17}$$

Later we show that in the large-n limit, equivalent to the limit $\xi\to 0$, the term $\hat{p}_{\xi,d}$ approaches a constant, $\hat{p}_{0,d}$. Hence, in the large-n limit the additive-sites approximation is equivalent to

$$q_n(\mathbf{r}|\mathbf{r}_0)\approx p_n(\mathbf{r}|\mathbf{r}_0)-\eta\,\frac{W_n(\mathbf{r}|\mathbf{r}_0;S)}{1+\eta(\hat{p}_{0,d}-1)}. \tag{2.18}$$

Our second observation is that correlations between different sites in S appear only in the terms $\hat{p}_{\xi,ij}$ in which $i\neq j$. A glance at Eqs. (2.15) and (2.16) indicates that these terms do not appear in the terms proportional to η in the numerator and denominator terms but do appear in the coefficients of η^2. Provided that suitable expressions for the $\hat{p}_{\xi,d}$ can be found, Eq. (2.12) can be used without further approximation to study frequency-domain spectroscopy by replacing ξ by $i\omega/(c\mu_s')$, where ω is the frequency, c is the speed of light in the slab, and μ_s' is the transport-corrected scattering factor. The form of the relation in Eq. (2.18) furnishes a simple and readily implementable approximation to $q_n(\mathbf{r}|\mathbf{r}_0)$. It can be shown to be accurate whenever the product $k\eta$ is small. This can sometimes be a realistic assumption for quite large clusters of anomalous sites. Recently published data on optical properties of both healthy and cancerous breast tissue in the near infrared indicates that the values of η may be as low as 0.001 [14,16], but more commonly are of the order of 0.01–0.02 [18].

C. Approximations to the generating functions

1. The additive-sites model

To draw further conclusions from the analysis we must specify usable approximations to the propagators that appear in Eqs. (2.5) and (2.6). For this purpose we note that translation of typical tissue slab widths into the integer units used in the random walk analysis suggest that these widths are typically of the order of 20–40 lattice spacings. Although it is possible to provide exact expressions for the propagators of the nearest-neighbor random walk used here [17], it is nevertheless convenient to work in terms of the Gaussian approximation, which is equivalent to taking n to be large. This is justified by the observation that n, in discrete units, must be at least as great as the slab width. To somewhat simplify the form of the resulting expressions we will distinguish between the variation between the (x,y) coordinates and the z coordinate by defining the two-dimensional vector $\boldsymbol{\rho}=(x,y)$, allowing us to express the vector $\mathbf{r}$ as $\mathbf{r}=(\boldsymbol{\rho},z)$.

The Gaussian approximation to the propagator in free space is

$$p_{n,\mathrm{FS}}(\mathbf{r}|\mathbf{r}_0)\approx\left(\frac{3}{2\pi n}\right)^{2/3}\exp\left[-\frac{3}{2n}\{(\boldsymbol{\rho}-\boldsymbol{\rho}_0)^2+(z-z_0)^2\}\right], \tag{2.19}$$

where $\boldsymbol{\rho}_0$ is the point in the (x,y) plane associated with $\mathbf{r}_0$. The posited physical picture requires that the boundaries at $z=0$ and $z=Z$ should consist only of absorbing points, which is equivalent to requiring that the boundary conditions

$$p_n(\boldsymbol{\rho},0|\mathbf{r}_0)=p_n(\boldsymbol{\rho},Z|\mathbf{r}_0)=0 \tag{2.20}$$

be satisfied. The propagator that takes into account absorbing boundaries is

$$p_n(\mathbf{r}|\mathbf{r}_0)\approx\delta_{\mathbf{r}\cdot\mathbf{r}_0}\delta_{n,0}+\left(\frac{3}{2\pi n}\right)^{3/2}\exp\left[-\frac{3}{2n}(\boldsymbol{\rho}-\boldsymbol{\rho}_0)^2\right]\sum_{j=-\infty}^{\infty}\left[\exp\left\{-\frac{3}{2n}(z-z_0+2jZ)^2\right\}-\exp\left\{-\frac{3}{2n}(z+z_0+2jZ)^2\right\}\right]. \tag{2.21}$$

An additional factor of $\delta_{\mathbf{r}\cdot\mathbf{r}_0}\delta_{n,0}$, corresponding to the initial condition, is included, since the calculation of $\hat{p}_{\xi,ii}$ requires that the behavior at $n=0$ should be correctly accounted for.

We will calculate an approximate but convenient form for the generating function $\hat{p}_\xi(\mathbf{r}|\mathbf{r}_0)$ by replacing the sum over n by an integral so that, for example,

$$\hat{p}_\xi(\mathbf{r}|\mathbf{r}_0)\approx\int_0^\infty e^{-\xi n}p_n(\mathbf{r}|\mathbf{r}_0)dn=\delta_{r,r_0}+\frac{3}{2\pi}\sum_{j=-\infty}^{\infty}[\hat{G}_\xi(\sqrt{(\boldsymbol{\rho}-\boldsymbol{\rho}_0)^2+(z-z_0+2jZ)^2})-\hat{G}_\xi(\sqrt{(\boldsymbol{\rho}-\boldsymbol{\rho}_0)^2+(z+z_0+2jZ)^2})], \tag{2.22}$$

where $\hat{G}_\xi(a)$ is the function

$$\hat{G}_\xi(a)=\frac{e^{-a\sqrt{6\xi}}}{a}. \tag{2.23}$$

Notice that the approximation in Eq. (2.22) cannot be used when $\mathbf{r}=\mathbf{r}_0$ since the term with $j=0$ will be infinite. Hence the evaluation of the self-terms $\hat{p}_{\xi,ii}=\hat{p}_\xi(\mathbf{s}_i|\mathbf{s}_i)$ requires a slight modification of the preceding analysis, which consists of accounting exactly for the $n=0$ term and setting the lower limit on the integral in Eq. (2.22) at $n=1$. Let z_i be the value of z in $\mathbf{s}_i$. We assume that z_i and Z are much greater than 1 and that $Z\gg z_i$, which means that an anomalous site is not too close to either of the boundaries. A consequence of this assumption is that the generating function $\hat{p}_{\xi,ii}$ is nearly independent of i. This assertion is based on retaining only the lowest order terms of the series in the expansion given in Eq. (2.22):

$$\hat{p}_{\xi,ii}\approx 1+\left(\frac{3}{2\pi}\right)^{3/2}\int_1^\infty\frac{e^{-\xi n}}{n^{3/2}}\,dn-\frac{3}{4\pi}\left\{\frac{e^{-z_i\sqrt{24\xi}}}{z_i}+\frac{e^{-(Z-z_i)\sqrt{24\xi}}}{Z-z_i}\right\}. \tag{2.24}$$

The dominant terms in this expression are the first two terms on the right-hand side, which are independent of i. The remaining terms in the infinite series have been dropped because they contain exponents in which Z appears with a coefficient greater than 1. Equation (2.24) indicates that when $\xi\approx 0$ the i-dependent terms are of order $1/z_i$, which causes an error of 5% or less for realistic choices of parameters. Hence, on setting $\xi=0$ we obtain an estimate $\hat{p}_{0,ii}-1\equiv\hat{p}_{0,d}\approx 0.66$. We can get a crude estimate of these approximations on the contrast function by replacing a term such as $\underline{p_l}(\mathbf{r}|\mathbf{s}_j)p_{n-l}(\mathbf{s}_j|\mathbf{r}_0)$ in Eq. (2.18) by $p_l(\mathbf{r}|\overline{\mathbf{s}})p_{n-l}(\overline{\mathbf{s}}|\mathbf{r}_0)$, where $\overline{\mathbf{s}}$ is a point in the center of the cluster (in fact, when the anomalous sites are sufficiently far from the absorbing boundaries the product does not vary significantly with their exact positions). With this further simplification we find

$$C_n(\boldsymbol{\rho};k)\approx\frac{k\eta}{1+0.66\eta}\,C_n(\boldsymbol{\rho};1), \tag{2.25}$$

where $C_n(\boldsymbol{\rho};1)$ is calculated as if there were a single anomalous site at $\overline{\mathbf{s}}$. Thus, in the additive-site approximation $C_n(\boldsymbol{\rho};k)$ is, to a first approximation, proportional to the number of anomalous sites.

2. Correlation effects

Corrections for correlation effects, i.e., inclusion of the terms proportional to η^2, must be made in both the numerator and denominator of Eq. (2.5). Consider first the specifics of the correction appearing in the denominator. We retain the assumption that the terms in the denominator do not depend on specific sites and can therefore be regarded as constants. Hence we make use of the small-ξ approximation to $\hat{p}_{\xi,ij}$ given in Eq. (2.22), which yields

$$\hat{p}_{0,ij}\approx\frac{3}{2\pi}\sum_{l=-\infty}^{\infty}\left\{\frac{1}{\sqrt{(\boldsymbol{\rho}_i-\boldsymbol{\rho}_j)^2+(z_i-z_j+2lZ)^2}}-\frac{1}{\sqrt{(\boldsymbol{\rho}_i-\boldsymbol{\rho}_j)^2+(z_i+z_j+2lZ)^2}}\right\},\quad i\neq j. \tag{2.26}$$

We calculate a few values of $\hat{p}_{0,ij}$ for $Z=41$ to give some idea of how these terms compare to the diagonal terms, which are all approximately equal to 0.66 provided that none of the sites is within one or two lattice units from an absorbing surface. First, if we assume that the anomalous sites are strung out along the z axis by setting $\boldsymbol{\rho}_i=\boldsymbol{\rho}_j$ and consider different values of z_i-z_j we find the values

z_i-z_j: (1) 0.46, (2) 0.22, (3) 0.14, (4) 0.10,

(5) 0.08, (6) 0.06.

These were calculated for points in the middle of a slab of thickness $Z=41$ and are roughly proportional to $1/|z_i-z_j|$. If the value of z is held constant so that the anomalous points are located in a plane the results obtained for differences measured along an axis in the plane of $\boldsymbol{\rho}$ are very closely equal to those just shown, again with the proviso that the anomalous points are close to the center of the slab.

One gets numbers similar to those just shown if one simultaneously varies the $\boldsymbol{\rho}$'s and z's. For example, if $|\boldsymbol{\rho}_i-\boldsymbol{\rho}_j|=|z_i-z_j|=1$, then $\hat{p}_{0,ij}=0.32$, which is only slightly

less than the results calculated for the nearest neighboring points as given above. Further numerical explorations indicate that the value of the $\{z_i\}$ has to be within two lattice units from the slab surfaces for there to be noticeable differences from the numbers shown. The results are essentially insensitive to the value of Z when $Z \geqslant 20$.

These considerations allow us to approximate the denominator term $\hat{D}(\xi,\eta)$ as

$$\hat{D}(\xi,\eta) \approx 1 + 0.66k\eta + \eta^2[(0.66)^2 k(k-1) - B] \tag{2.27}$$

in which

$$\mathbf{r} = (\boldsymbol{\rho}, Z-1) \quad \text{and} \quad B = \sum_{j=1}^{k} \sum_{i(\neq)j=1}^{k} \hat{p}^2_{0,ij}. \tag{2.28}$$

To the order of the approximation shown, the effect of correlations in the denominator of Eq. (2.5) appears only in the single term B defined in Eq. (2.28) which is therefore to be compared to the term $(0.66)^2 k(k-1)$. For a cube of $3\times3\times3$ points, centered at $z=10$ with $Z=21$ the value of B is equal to 16% of the first term in square brackets. Thus, when η is large enough that the η^2 term gives a noticeable contribution to the contrast but the η^3 term can be ignored, the correlation correction to the η^2 term is small but not entirely negligible. Also, since B is positive, the effect of correlations in the present approximation is to enhance the contrast. For the slightly larger cube of points, $5\times5\times5$, likewise centered at $z=10$, the value of B is 6.4% of the term $(0.66)^2 k(k-1)$. These results suggest that body shape becomes less important in determining contrast as the size of the body increases.

III. SOME NUMERICAL CALCULATIONS

A. The contrast function in discrete time

Numerical calculations are required to determine the order of magnitude of correlation effects in the numerator of Eq. (2.5) as found from the second-order term in Eq. (2.16). To simplify these calculations for terms appearing in the function $W_n(\mathbf{r}|\mathbf{r}_0)$ we make use of the approximation

$$\sum_{l=0}^{n} p_l(\mathbf{s}_j|\mathbf{r}_0) p_{n-l}(\mathbf{r}|\mathbf{s}_j) \approx \int_0^{n+1} p_l(\mathbf{s}_j|\mathbf{r}_0) p_{n+1-l}(\mathbf{r}|\mathbf{s}_j)\, dl. \tag{3.1}$$

This is consistent with our use of a large-n approximation to the propagator. The factor n in the sum has been replaced by $n+1$ in the integral to reconcile the use of the Gaussian propagator, i.e., one that describes motion in a continuum, with a lattice formulation. This accounts for the fact that the theory actually calculates a first-passage time to the point $\mathbf{r}$. The sum on left-hand side of Eq. (3.1) refers to the trajectory to a site at $z=Z-1$ while the propagator in the Gaussian approximation refers to a continuum picture, which takes the photon to $z=Z$. To compensate for this difference we have replaced n by $n+1$ on the right-hand side of the equation. That this provides a qualitatively more accurate solution has been checked using the technique of exact enumeration, which provides a solution to the lattice problem exact to within the number of digits available for the computation [19,20].

We have carried out numerical calculations to compare the contrast function predicted by the additive-sites model in Eq. (2.18), which has no correlation terms to the lowest order approximation that does, which combines Eq. (2.16) and (2.27) and substitutes the result into Eq. (2.5). To this order of approximation the contrast function can be written as

$$C_n(\boldsymbol{\rho};k) \approx \eta \frac{[1+0.66(k-1)\eta] W_n(\mathbf{r}|\mathbf{r}_0;S) - \eta U_n(\mathbf{r}|\mathbf{r}_0;S)}{1+0.66k\eta+\eta^2[(0.66)^2 k(k-1)-B]} \tag{3.2}$$

in which $U_n(\mathbf{r}|\mathbf{r}_0)$ is the inverse transform

$$U_n(\mathbf{r}|\mathbf{r}_0;S) = \mathcal{L}^{-1}\left\{ \sum_{i(\neq j)=1}^{k} \sum_{j=1}^{k} \hat{p}_\xi(\mathbf{r}|\mathbf{s}_j)\hat{p}_\xi(\mathbf{s}_j|\mathbf{s}_i)\hat{p}_\xi(\mathbf{s}_i|\mathbf{r}_0) \right\}. \tag{3.3}$$

To simplify calculations we discuss properties of $C_n(\boldsymbol{\rho};k)$ for a coaxial beam passing through the center of the cubic cluster, as shown in Fig. 1.

In the large-n regime the value of $W_n(\mathbf{r}|\mathbf{r}_0;S)$ can be written as

$$W_n(\mathbf{r}|\mathbf{r}_0;S) \approx \left(\frac{3}{2\pi}\right)^{5/2} \sum_{j=1}^{k} \sum_{l=-\infty}^{\infty} \sum_{l'=-\infty}^{\infty} [G_n^{++}(l,l') + G_n^{--}(l,l') - G_n^{+-}(l,l') - G_n^{-+}(l,l')] \tag{3.4}$$

in which, for example,

$$G_n^{+-}(l,l') = \frac{1}{n^{3/2}} \left(\frac{1}{a_l^+} + \frac{1}{b_{l'}^-}\right) \exp\left[-\frac{3}{2n}(a_l^+ + b_{l'}^-)^2\right], \tag{3.5}$$

where

$$a_l^\pm = \sqrt{\rho_j^2 + (z_j \pm 1 + 2lZ)^2}, \qquad b_l^\pm = \sqrt{\rho_j^2 + (Z-1\pm z_j + 2lZ)^2}. \tag{3.6}$$

The function $U_n(\mathbf{r}|\mathbf{r}_0;S)$ that appears in Eq. (3.2) has the slightly more complicated form

$$\begin{aligned} U_n(\mathbf{r}|\mathbf{r}_0;S) \approx{}& \left(\frac{3}{2\pi}\right)^{7/2} \sum_{j=1}^{k} \sum_{i(\neq j)=1}^{k} \sum_{l=-\infty}^{\infty} \sum_{l'=-\infty}^{\infty} \sum_{l''=-\infty}^{\infty} [H_n^{---}(\cdot) \\ &+ H_n^{++-}(\cdot) + H_n^{+-+}(\cdot) + H_n^{-++}(\cdot) - H_n^{+++}(\cdot) \\ &- H_n^{+--}(\cdot) - H_n^{-+-}(\cdot) - H_n^{--+}(\cdot)]. \end{aligned} \tag{3.7}$$

The H_n functions that appear here have a form exemplified by

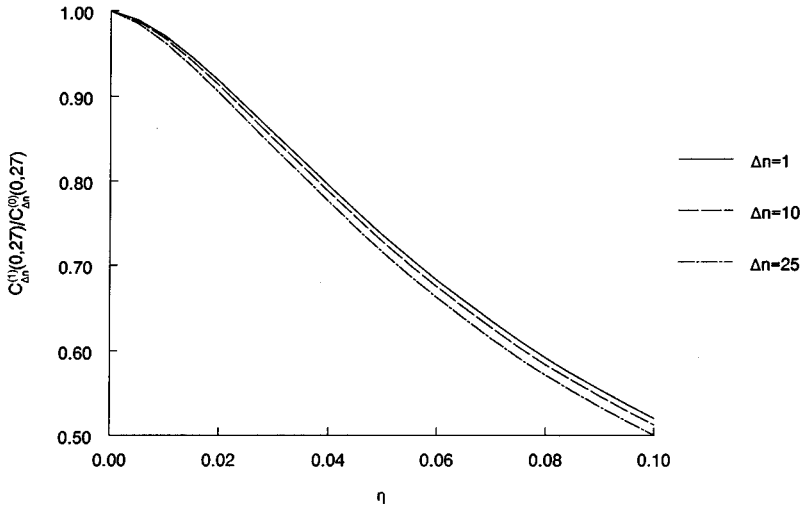

FIG. 2. The ratio of contrasts with and without the first-order correction for a cube of $3\times3\times3$ points in a slab of $Z=21$ sites. Calculations were made only for the coaxial configuration in which $\mathbf{r}_0=(0,0,1)$, $\mathbf{r}=(0,0,20)$, the cube being centered at (0,0,10).

$$H_n^{+\,+\,-}(l,l',l'')=\frac{1}{n^{3/2}}\left(\frac{1}{a_l^+ b_{l'}^+}+\frac{1}{b_{l'}^+ c_{l''}^-}+\frac{1}{c_{l''}^- a_l^+}\right)\times\exp\left[-\frac{3}{2n}\,(a_l^+ + b_{l'}^+ + c_{l''}^-)^2\right] \quad (3.8)$$

in which, in addition to the variables $a_l^{\pm}$ and $b_l^{\pm}$ defined in Eq. (3.6) we have also used

$$c_l^{\pm}=\sqrt{\rho_j^2+(Z-1\pm z_j+2lZ)^2}. \quad (3.9)$$

Derivations of Eqs. (3.4) and (3.7) are given in the Appendix.

A comparison of results obtained using the additive-sites model [Eq. (2.18)] and the first-order correction in Eq. (3.2) is shown in Fig. 2. Let $C_{\Delta n}^{(1)}(0,27;\eta)$ denote the first-order corrected contrast function for 27 anomalous points arranged in a cube and let $C_{\Delta n}^{(0)}(0,27;\eta)$ be the contrast function in the additive-sites approximation. The curves in Fig. 2 are of the ratio $C_{\Delta n}^{(1)}(0,27;\eta)/C_{\Delta n}^{(0)}(0,27;\eta)$ plotted as a function of the absorption probability η. When $\eta=0$ the ratio is equal to 1 and is seen to increase as η increases. The increase at small η reflects the fact that a photon generally must visit several sites before being absorbed, thereby emphasizing the importance of correlation terms. When η is close to 1 the photon is most likely to be absorbed at the first anomalous site visited, hence correlations tend to be less significant. This effect is reflected in the slight decrease in $C_{\Delta n}^{(1)}(0,27;\eta)/C_{\Delta n}^{(0)}(0,27;\eta)$ observed at the larger values of η in Fig. 2. To further examine correlation effects we have also calculated the value η', which is the solution to

$$C_1^{(0)}(0,27;\eta')=C_1^{(1)}(0,27;\eta). \quad (3.10)$$

That is to say, we calculate the absorption probability required to bring the additive-sites model into coincidence with a model taking correlations into account. The results are plotted in Fig. 3. Although we have chosen $\Delta n=1$, increasing the value of the time changes the results by only an insignificant amount so that Fig. 3 can be considered typical. We see that at values of η less than 0.015, to a good approximation $\eta'=\eta$. The deviations become much more noticeable at larger values of the absorption. For example, at $\eta=0.02$ the relative discrepancy between the two approximate results is 8.4% and at $\eta=0.03$ it is 14.6%. Whether this is to be considered an accurate approximation would depend on the magnitude of measurement error. With a smaller number of anomalous points $\eta'\approx\eta$ over a greater range of η.

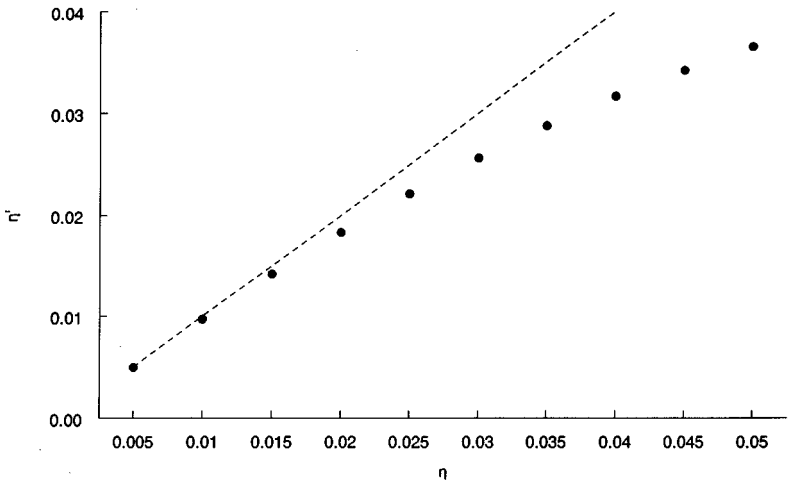

FIG. 3. A plot of η', which is generated from the equation $C_1^{(0)}(0,27;\eta')=C_1^{(1)}(0,27;\eta)$. The straight line is $\eta'=\eta$ and the points indicate that $\eta'<\eta$ whenever η differs from 0.

B. Conversion of dimensionless units to physical ones

While our theoretical results are expressed in terms of lattice units for both space and time, they are readily converted to physical units. These will be denoted by a bar over the symbol, so that $\overline{z}$ is a physical length that corresponds to the dimensionless coordinate z. The relation between the dimensionless and physical spatial variables is

$$\overline{z} = z\mu_s'/\sqrt{2}, \tag{3.11}$$

where μ_s' is the transport-corrected scattering coefficient [18]. Let c be the speed of light in the medium. Then the time in physical units can be related to the discrete time n by $t = n/(c\mu_s')$. If the absorption coefficient is denoted by μ_a then, as noted in [11], to a good approximation the parameter η is given by $\eta = \mu_a/\mu_s'$.

IV. DISCUSSION

Our calculations presume that the absorption probability at a single site is small, as is generally true for transillumination experiments that use NIR radiation. This circumstance allows us to develop a perturbation expansion that greatly simplifies the evaluation of the determinants in the exact expression in Eq. (2.5). The results obtained using this formalism suggest that at physiologically realistic values of the absorption probability it would be difficult to distinguish between different configurations of clusters of anomalous sites. This tends to support the analysis proposed in [9] in which only a single site was used to derive results that were then applied to nonlocal clusters of anomalous points. Whether an approximation based on replacing several sites by a single one is also useful when η is not small has not yet been addressed to our knowledge. If η is close to 1 it is unclear whether the use of random walk theory using the large-n approximation in Eq. (2.21) is still an appropriate one to use.

Finally, the present paper considers only anomalous behavior expressible in terms of absorption. A similar formalism can be developed when the anomaly occurs in the scattering coefficient, or in both. The formalism required to analyze this more general case has recently been developed in another context in [21]. An alternative formalism for incorporating anomalous scattering into the general analysis is given in [22]. A further feature easily incorporated into the formalism is one in which the normal points also allow for absorption. This has not been included in the present report.

Work is presently in progress on recasting the random walk theory in terms of the continuous-time random walk [10], which simplifies many features of the theory. The results will be reported elsewhere.

ACKNOWLEDGEMENTS

We are grateful to Dr. Victor Chernomordik and Dr. Ralph Nossal for their careful reading of this paper and for several useful comments.

APPENDIX: FORMULA USED TO CALCULATE THE CONTRAST FUNCTIONS

The formula for $W_n(\mathbf{r}|\mathbf{r}_0)$ is found by substituting the propagator in Eq. (2.21) into Eq. (3.1). It will be expressed in terms of a function $G_n(a,b)$ defined by

$$G_n(a,b) = \frac{1}{n^{3/2}}\left(\frac{1}{\sqrt{a}}+\frac{1}{\sqrt{b}}\right)\exp\left[-\frac{3}{2n}(\sqrt{a}+\sqrt{b})^2\right] \tag{A1}$$

and the variables

$$\begin{aligned}\alpha_\pm(j,m) &= (\boldsymbol{\rho}_j-\boldsymbol{\rho})^2+[s_j(z)\pm 1+2mZ]^2,\\ \beta_\pm(j,m') &= (\boldsymbol{\rho}_j-\boldsymbol{\rho})^2+[(2m'+1)Z-1\pm s_j(z)]^2.\end{aligned} \tag{A2}$$

The contrast function for a single site is now written as

$$C_n(\boldsymbol{\rho};1) = \left(\frac{3}{2\pi}\right)\frac{\sum_{m=-\infty}^{\infty}\sum_{m'=-\infty}^{\infty}[G_n(\alpha_+,\beta_+)+G_n(\alpha_-,\beta_-)-G_n(\alpha_+,\beta_-)-G_n(\alpha_-,\beta_+)]}{\sum_{m=-\infty}^{\infty}(\exp\{-3[(2m+1)Z-2]^2/2n\}-\exp[-3(2m+1)^2Z^2/2n])}, \tag{A3}$$

which has been used to generate the curves described in the text. The formula in Eq. (A1) has been generated by multiplying appropriate transforms $\hat{G}_\xi(a)$ as defined in Eq. (2.23) together according to the expansion provided by the method of images, and finally inverting the result. A similar method has been used to generate the functions H_n that appear in Eqs. (3.7) and (3.8).

[1] *Optical Tomography, Photon Migration, and Spectroscopy of Tissue and Model Media*, edited by B. Chance and R. R. Alfano, Proc. SPIE No. 2389 (SPIE, Bellingham, 1995).

[2] B. B. Das, F. Liu, and R. R. Alfano, Rep. Prog. Phys. **60**, 227 (1997).

[3] S. R. Arridge, P. van der Zee, M. Cope, and D. T. Delpy, Proc. SPIE **1431**, 204 (1991).

[4] R. L. Barbour, H. L. Graber, Y. Wang, J. H. Chang, and R. Aronson, Proc. SPIE **IS11**, 87 (1993).

[5] W. Zhu, Y. Wang, J. Chang, H. L. Graber, and R. L. Barbour, Proc. SPIE **2389**, 420 (1995).

[6] P. N. den Outer, Th. M. Niewenhuizen, and A. Lagendijk, J. Opt. Soc. Am. A **10**, 1209 (1993).

[7] R. F. Bonner, R. J. Nossal, S. Havlin, and G. H. Weiss, J. Opt. Soc. Am. A **4**, 423 (1987).

[8] A. H. Gandjbakhche and G. H. Weiss, Prog. Opt. **34**, 333 (1995).

[9] A. H. Gandjbackhche, V. Chernomordik, R. F. Bonner, R.

Nossal, G. H. Weiss, and J. Hebden, in *Trends in Optics and Photonics*, edited by R. R. Alfano and J. G. Fujimoto (Optical Society of America, Washington, D.C., 1996), Vol. 2, p. 183.
[10] G. H. Weiss, *Aspects and Applications of the Random Walk*, North-Holland, Amsterdam, 1994.
[11] A. H. Gandjbakhche, R. F. Bonner, R. Nossal, and G. H. Weiss, Appl. Opt. **35**, 1767 (1996).
[12] A. H. Gandjbakhche, R. F. Bonner, I. Gannot, J. Knutson, R. Navai, R. Nossal, and G. H. Weiss, Proc. SPIE **2679**, 8 (1996).
[13] A. H. Gandjbakhche, R. F. Bonner, R. Nossal, and G. H. Weiss, Appl. Opt. **36**, 4613 (1997).
[14] T. L. Troy, D. L. Page, and E. M. Sevick-Muraca, J. Biomed. Opt. **1**, 342 (1996).
[15] R. J. Rubin and G. H. Weiss, J. Math. Phys. (N.Y.) **23**, 250 (1982).
[16] H. Heusmann, J. Kölzer, and G. Mitic, J. Biomed. Opt. **1**, 425 (1996).
[17] A. H. Gandjbakhche, G. H. Weiss, R. F. Bonner, and R. Nossal, Phys. Rev. E **48**, 810 (1993).
[18] V. G. Peters, D. R. Wyman, M. S. Patterson, and G. L. Frank, Phys. Med. Biol. **35**, 1317 (1990).
[19] D. ben-Avraham and S. Havlin, J. Phys. A **15**, 691 (1982).
[20] S. Havlin, J. E. Kiefer, B. Trus, G. H. Weiss, and R. Nossal, Appl. Opt. **32**, 617 (1993).
[21] G. H. Weiss and P. P. Calabrese, Physica A **234**, 443 (1996).
[22] A. H. Gandjbakhche, V. Chernomordik, R. F. Bonner, J. C. Hebden, and R. Nossal, Proc. SPIE (to be published).